Published in final edited form as:
Cell Rep. 2016 April 12; 15(2): 336–348. doi:10.1016/j.celrep.2016.03.020.

Tumor-Induced Hyperlipidemia Contributes to Tumor Growth

Jianfeng Huang[1,2], **Lena Li**[2,3], **Jihong Lian**[2,3], **Silvia Schauer**[1], **Paul W. Vesely**[1,5], **Dagmar Kratky**[4], **Gerald Hoefler**[1,*], and **Richard Lehner**[2,3,*]

[1]Institute of Pathology, Medical University of Graz, 8010 Graz, Austria

[2]Group on Molecular and Cell Biology of Lipids

[3]Department of Pediatrics, University of Alberta, Edmonton, AB T6G 2R3, Canada

[4]Institute of Molecular Biology and Biochemistry, Center of Molecular Medicine, Medical University of Graz, 8010 Graz, Austria

[5]Institute of Molecular Biosciences, Karl Franzens University of Graz, 8010 Graz, Austria

Summary

The known link between obesity and cancer suggests an important interaction between the host lipid metabolism and tumorigenesis. Here, we used a syngeneic tumor graft model to demonstrate that tumor development influences the host lipid metabolism. BCR-Abl-transformed precursor B cell tumors induced hyperlipidemia by stimulating very low-density lipoprotein (VLDL) production and blunting VLDL and low-density lipoprotein (LDL) turnover. To assess whether tumor progression was dependent on tumor-induced hyperlipidemia, we utilized the VLDL production-deficient mouse model, carboxylesterase3/triacylglycerol hydrolase (Ces3/TGH) knockout mice. In Ces3/Tgh$^{-/-}$ tumor-bearing mice, plasma triglyceride and cholesterol levels were attenuated. Importantly tumor weight was reduced in *Ces3/Tgh*$^{-/-}$ mice. Mechanistically, reduced tumor growth in Ces3/Tgh$^{-/-}$ mice was attributed to reversal of tumor-induced PCSK9-mediated degradation of hepatic LDLR and decrease of LDL turnover. Our data demonstrate that tumor-induced hyperlipidemia encompasses a feed-forward loop that reprograms hepatic lipoprotein homeostasis in part by providing LDL cholesterol to support tumor growth.

Introduction

Dyslipidemia is tightly linked to obesity and is characterized by high levels of triacylglycerol (TG) and low-density lipoprotein cholesterol (LDL-C) as well as low levels of high-density lipoprotein cholesterol (HDL-C) in the bloodstream. Dyslipidimia is also associated with increased human cancer mortality (Calle et al., 2003). This has been functionally validated in experimental models of diet-induced obesity (DIO) that showed poor cancer outcomes (Alikhani et al., 2013; Zhuang et al., 2005). Weight loss intervention has been suggested as an effective cancer prevention strategy and is supported by reductions in cancer incidence and mortality of patients who have had bariatric surgery and dramatic

*Correspondence: gerald.hoefler@medunigraz.at (G.H.), richard.lehner@ualberata.ca (R.L.).

Europe PMC Funders Author Manuscripts

weight loss (Sjöström et al., 2009). However, whether nonsurgical weight loss interventions achieved by calorie restriction, behavioral therapy, and/or pharmacotherapy could also have a beneficial impact on cancer incidence is still unclear. Mechanistic investigations into this relationship have analyzed the potential roles of insulin, insulin-like growth factors (IGFs), sex hormones, and adipokines (e.g., leptin, tumor necrosis factor alpha [TNF-α], and adiponectin). Plasma concentrations of these are often abnormal in obesity (Al-Zoughbi et al., 2014). Onset of insulin resistance and chronic inflammation resulting from excess lipid supply and adipose expansion can distort the normal balance between cell proliferation and differentiation and apoptosis, which eventually contribute to obesity-induced cancer incidence (Bianchini et al., 2002). However, the precise cellular mechanisms that link obesity with cancer incidence, recurrence, progression and death remain largely unexplored. Furthermore, whether dyslipidemia in normal-weight subjects is correlated to tumor incidence is unknown.

Rapidly proliferating tumor cells generally require high amounts of fatty acids (FAs) and cholesterol. Numerous studies have confirmed hyperactivation of de novo lipogenesis in various types of neoplasia. Targeting lipogenesis by inhibiting fatty acid synthase (FASN), stearoyl-CoA desaturase-1 (SCD1), ATP-citrate lyase (ACLY) or sterol regulatory element-binding protein-1 (SREBP1) was effective in tumor suppression (Currie et al., 2013). Cancer cells can also rapidly convert exogenous FAs to lipids required for proliferation and pro-tumorigenic lipid signaling (Arana et al., 2010; Louie et al., 2013). Multiple studies have also demonstrated elevated low-density lipoprotein (LDL) receptor (LDLR) expression and LDL uptake in a wide range of tumors, including glioblastoma (Guo et al., 2011), leukemia (Vitols et al., 1990), pancreatic tumors (Guillaumond et al., 2015), and lung cancer (Vitols et al., 1992). Lipoprotein lipase (LPL), which hydrolyzes TG within chylomicrons (CM) and very low-density lipoprotein (VLDL), was found to be critical for cancer cells to acquire FA from culture medium (Kuemmerle et al., 2011).

To elucidate a potential role of VLDL-derived lipids in tumorigenesis in vivo, we studied tumor growth in a mouse model with attenuated VLDL production: carboxylesterase 3/triacylglycerol hydrolase (Ces3/TGH) deficient (−/−) mice. Ces3/TGH (annotated as carboxylesterase 1 [CES1] in humans) promotes VLDL assembly and secretion (Dolinsky et al., 2004a, 2004b). Mice lacking Ces3/TGH display reduced ApoB and TG in plasma when fed chow or Western-type diets (Lian et al., 2012a, 2012b; Wei et al., 2010).

In this study, we explored (1) whether BCR-Abl-transformed B cell tumors modulate lipoprotein homeostasis and (2) how insufficient supply of circulating lipids influenced tumor growth in mice. We demonstrate that *Ces3/Tgh*$^{-/-}$ mice are resistant to tumor-induced downregulation of LDLR in liver, tumor-induced hyperlipidemia and, consequently, have significantly reduced tumor growth.

Results

Lipoproteins Are Essential for Growth and Survival of Transformed B Cells In Vitro

To investigate whether tumor cell growth depends on exogenous lipid supply, we used tumorigenic, rapidly proliferating BCR-Abl-transformed precursor B cells (TPBCs) as a

tumor model (Huang et al., 2013). Incubation of cells in medium containing lipoprotein-deficient serum (LPDS) resulted in significant growth inhibition and increased cell death. Supplementation of LPDS with VLDL, LDL, or HDL partially restored the rapid growth rate of TPBCs (Figures 1A and 1B) and prevented cell death in a dose-dependent manner (Figure S1A). Protection against lipid depletion-induced cell death was achieved when tumor cells were supplied with acetylated LDL, which requires scavenger receptors, but not LDLR, for internalization (Figure S1B). Importantly, cholesterol addition alone was able to restore cell proliferation and alleviate cell death (Figures 1A, 1B, and S1A). The increased apoptotic rate confirmed that severe cell damage occurred upon lipid withdrawal, which could be reversed by re-supplying lipoproteins or cholesterol. To further confirm the role of cholesterol in tumor cell growth, we used three pharmacological approaches (Figure 1D) to prevent its utilization by tumor cells (Figure 1C): (1) depletion of cell membrane cholesterol by cyclodextrin (HPCD), (2) inhibition of cholesterol synthesis and intake by blockage of the SREBP pathway using fatostatin, and (3) abolishment of lysosomal hydrolysis of endocytosed VLDL remnant/LDL cholesteryl esters (CEs) by NH_4Cl. All conditions significantly suppressed TPBC growth (Figures 1E–1G). To investigate the mechanism by which tumor cells take up lipids from lipoproteins, we examined quantitative transcriptional expression of genes involved in TG hydrolysis and lipid transport. Interestingly, mRNA expression of *Ldlr* was 50-fold higher than VLDL receptor (*Vldlr*) (Figure 1H). *Ldlrap1*, which encodes a protein that is involved in internalization of LDL-bound LDLR, was also substantially expressed. This finding suggests that LDLR might play a major role in facilitating lipoprotein uptake by tumors (schematic depiction in Figure 1D). Lipoprotein-receptor-related proteins and scavenger receptors might also play a role in lipoprotein uptake. Thus, we determined mRNA expression of important candidates and found *Lrp10* to be highly expressed (Figure S1C). LRP10 is reportedly involved in ApoE-containing lipoprotein uptake, whereas SR-B1 facilitates HDL uptake. Regarding FA uptake, we found *Fabp5* and *Slc27a4* mRNA to be highly abundant in tumors. Indeed, supplementation of LPDS with oleate increased growth of TPBCs in LPDS (Figure S1D). Thus, TPBC-dependence on lipoproteins was associated with elevated expression of genes involved in LDL internalization, ApoE-specific lipoprotein uptake, and FA uptake.

Because it has been reported that LDLR is overexpressed in several types of tumor, we were particularly interested to investigate the potential regulatory mechanism of LDLR expression in cancer. In healthy cells, *Ldlr* mRNA expression is under the control of SREBPs. Here, we analyzed expression correlation based on mRNA profiles obtained from the Cancer Genome Atlas Project (TCGA). We found that *Ldlr* mRNA levels are significantly correlated to *Srebp1* and *2* as well as their target genes in a wide range of human cancer types, including diffuse large B cell lymphoma (Table S1). These correlations imply that *Ldlr* is transcriptionally regulated by both SREBPs and might share similar expression patterns with other SREBPs target genes in cancers.

TPBC Tumor Grafts Induce Hyperlipidemia by Increasing VLDL Production and Decreasing CM/VLDL Turnover

We next investigated whether tumor tissue altered lipid homeostasis in C57BL6 mice injected with TPBC cells in the subcutaneous flank. Elevated plasma TG and TC

concentrations and correspondingly increased VLDL and LDL levels were detected in tumor-bearing versus control *WT* mice (Figures 2A and S2A). To specifically investigate the mechanism of enhanced VLDL production, we repeated the experiment in *Ldlr*$^{-/-}$ mice, a hyperlipidemic mouse model deficient in LDL clearance. An even more pronounced increase of VLDL and LDL was observed in these tumor-bearing mice, suggesting that upregulation of VLDL production was responsible for the increase in VLDL and LDL levels (Figures 2A and S2A). Fasting plasma non-esterified FA (NEFA) concentrations, representing adipose tissue TG catabolism and FA supply for hepatic VLDL assembly, were similar in tumor-bearing and control mice (Figure S2B), suggesting mechanism other than substrate availability. We therefore investigated the possible mechanisms for tumor-directed increased levels of circulating VLDL by examining VLDL synthesis in the liver. In the tumor-bearing group, however, hepatic TG and free cholesterol (FC) levels were decreased by 49.5% (Figure 2B) and 34.3% (Figure S2C), respectively. Correspondingly, the number of cytosolic lipid droplets in hepatocytes was also reduced in the tumor-bearing group (Figure 2C). Hepatic microsomal triglyceride transfer protein (Mttp), ApoB, and ApoE were similar between the tumor- and non-tumor-bearing groups (Figure S2D). These results indicated that tumor growth stimulated VLDL secretion.

Because augmented hepatic de novo lipogenesis increases VLDL secretion we investigated whether lipogenesis might be affected by the tumor. Primary hepatocytes isolated from tumor-bearing mice incorporated 2.4-fold and 1.8-fold more [^{3}H] acetate into FC and CEs, respectively (Figure 2D) and 1.3-fold more [^{3}H] oleate into TG (Figure 2E). The excess supply of intracellular cholesterol resulted in 3.0-fold increased esterification of [^{3}H] oleate into CE in hepatocytes from tumor-bearing mice (Figure 2E). Moreover, reduced intracellular labeling in de novo synthesized FA suggests enhanced FA channeling into CE and TG in livers of tumor-bearing mice (Figures 2D and 2E). The increased intracellular TG and cholesterol pool may support increased secretion of lipids in ApoB-containing lipoproteins. However, the observed enhanced secretion of TG was normalized after withdrawal of exogenous FA (Figure 2F), suggesting that the tumor enhances secretion of newly synthesized rather than preformed TG. Acid soluble metabolites (ASMs) derived from [^{3}H] oleate via FA oxidation were decreased in the tumor-bearing group (Figure S2E), which could provide an alternative FA source for TG and CE synthesis.

Next, we performed a fat tolerance test (FTT), which revealed that tumor-bearing mice accumulated 1.9-fold more CM-TG in plasma (Figure 2G), indicating impaired turnover of TG-rich lipoproteins by the tumor. Interestingly, comparable amounts of radioactivity were found in tumor and white adipose tissue (WAT) (Figure S2F), suggesting rapid and substantial lipoprotein lipase (LPL)-mediated uptake of CM-derived lipids by the tumor in mice with increased availability of circulating CM due to impaired TG turnover.

TPBC Tumors Decrease Hepatic LDLR Protein Expression, but Not Its Transcription

Hepatic LDLR protein abundance inversely correlates with plasma LDL concentrations. The amount of hepatic LDLR was significantly reduced in non-fasted tumor-bearing mice (Figure 3A), explaining in part the elevated LDL levels in these animals. To investigate the mechanism of this difference in LDLR abundance, we examined the transcriptional

expression and processing of the upstream regulators SREBP1 and 2 between control and tumor-bearing mice. In non-fasted mice, along with decreased LDLR protein expression (−64.7%), the precursor and mature SREBP1 were reduced by 49.1% and 53.8%, respectively, whereas the SREBP2 precursor was unaffected (Figure 3A). mRNA expression of *Fbxw7*, which catalyzes the ubiquitination of ER-localized SREBPs and promotes their subsequent degradation, was upregulated in tumor-bearing mice, whereas mRNA expression of *Insig2*, *Scap*, and *Mbtps1* encoding proteins involved in SREBP processing was unchanged (Figure 3B). Unexpectedly, except for mRNA expression of *Pcsk9*, which encodes a protein that is mainly synthesized and secreted from liver and induces degradation of hepatic LDLR, expression of other SREBP target genes, including *Ldlr*, was unchanged in tumor-bearing mice (Figure 3C). In concert, protein levels of FASN, acetyl coenzyme A (acetyl-CoA) carboxylase (ACC) 1 and 2, and 3-hydroxy-3-methylglutary-CoA reductase (HMGCR) were also unaltered (Figure 3D). The comparatively low levels of LDLR in tumor-bearing mice persisted even during overnight fasting (−59.1%; Figure 3E) and after refeeding (−41.5%; Figure 3F), regardless of the reported absence of mature SREBPs during fasting (Horton et al., 1998). Further analyses of mRNA expression resulted in expected pattern of expression of SREBPs target genes except for *Pcsk9* during fasting and refeeding (Figure 3G). Accordingly, plasma PCSK9 concentrations were dramatically elevated in tumor-bearing mice (Figures 3H and 3I). These results suggest that the downregulation of LDLR protein levels in TPBC tumor-bearing mice is independent of SREBP signaling but dependent on PCSK9. In addition, we detected similar concentrations of plasma PCSK9 in mice bearing lung carcinoma LLC (21 days) as those in mice bearing TPBCs (14 days) (Figure 3H), which were associated with a marked elevation of plasma VLDL, LDL (Figures 3J and S3A), and TC (Figure S3B) in LLC mice. In contrast, the increase in plasma PCSK9 concentration was moderate in mice bearing melanoma B16 (17 days) (Figure 3I) and was accompanied by only a marginal increase of LDL, HDL (Figures 3K and S3C), and TC (Figure S3D). Interestingly, expression of hepatic *Pcsk9* and other SREBP target genes was downregulated in both LLC and melanoma B16 groups (Figure S3E), although hepatic LDLR protein remained unchanged (Figure S3F).

Unaltered Insulin Sensitivity in TPBC Tumor-Induced Hyperlipidemia

Dyslipidemia is often associated with chronic inflammation and insulin resistance (IR), which has been proposed as a mechanistic link between cancer and obesity. Thus, we studied whether TPBC tumor-induced hyperlipidemia could also induce IR in our experimental model by measuring insulin sensitivity in liver and skeletal muscle. Basal AKT phosphorylation in livers of tumor-bearing mice was higher, whereas insulin-stimulated AKT activation was comparable to control mice (Figure 4A). Basal and stimulated AKT phosphorylation in muscle was unchanged (Figure 4A). In line with similar insulin sensitivity between the two models, an oral glucose tolerant test (OGTT) and insulin tolerant test (ITT) also revealed no changes between tumor-bearing and control mice (Figures 4B and 4C). Indeed, the tumorigenic cytokine IGF-1, the bioactivity of which is increased during IR, failed to stimulate TPBC growth in vitro (Figure S4A). Interestingly, blood glucose levels after overnight fasting and in non-fasted conditions were significantly lower in tumor-bearing mice (Figure S4B), which could be due to accelerated glucose uptake by the tumor, but not to improved global insulin sensitivity.

Attenuated TPBC Tumor-Induced Hyperlipidemia and Tumor Growth in *Ces3/Tgh*$^{-/-}$ Mice

We hypothesized that TPBC tumor-induced hyperlipidemia might provide excess amounts of cholesterol to stimulate tumor cell growth. Therefore, we utilized the genetic hypolipidemic mouse model—Ces3/TGH knockout mice (*Ces3/Tgh*$^{-/-}$)—to determine whether attenuated VLDL secretion could reverse tumor-induced hyperlipidemia and consequently suppress tumor growth. While food intake is similar in wild-type (WT) *and Ces3/Tgh*$^{-/-}$ mice (Figure S5A), plasma TG concentrations were decreased by 34.6% in *Ces3/Tgh*$^{-/-}$ mice (Figure 5A), with concomitantly significantly reduced plasma ApoB100 (Figure 5C), a marker of VLDL and LDL. In tumor-bearing *Ces3/Tgh*$^{-/-}$ mice, plasma TG levels remained reduced by 32.4% (Figure 5A) and cholesterol was lower in VLDL and LDL fractions (Figure 5B, right: FPLC), while plasma total cholesterol (TC) concentrations were lower by 15% (Figure 5B) in *Ces3/Tgh*$^{-/-}$ compared to WT, mice regardless of augmented HDL-C. Plasma NEFA concentrations were reduced in *Ces3/Tgh*$^{-/-}$ mice, but not in tumor-bearing *Ces3/Tgh*$^{-/-}$ mice (Figure S5B). The abundance of ApoB100 was profoundly lower in tumor-bearing *Ces3/Tgh*$^{-/-}$ mice compared to tumor-bearing WT mice (Figure 5C). Interestingly, tumor volume at 13 to 14 days post-inoculation and tumor weight 14 days after inoculation were reduced by 45.5% and 35.7% in *Ces3/Tgh*$^{-/-}$ mice, respectively (Figures 5D and 5E). Similarly, carcass body weight gain was also reduced in *Ces3/Tgh*$^{-/-}$ mice (Figure S5C). Attenuation of tumor-induced hyperlipidemia consequently caused a reduction in tumor TG (74.1%), FC (23%), and CE (22.9%) and a trend toward decreased tumor NEFA concentrations (62.5%, $p = 0.28$) in *Ces3/Tgh*$^{-/-}$ versus WT mice (Figures 5F–5H). Protein abundance of FASN and HMGCR were unchanged in tumors of *Ces3/Tgh*$^{-/-}$ mice. Increased expression of LDLR in tumors of *Ces3/Tgh*$^{-/-}$ mice, however, might at least in part compensate for the reduced availability of cholesterol (Figure 5I).

Consistent with enhanced TG secretion from primary hepatocytes of tumor-bearing mice (Figures 2E and 2F), VLDL secretion (determined at day 14) was significantly increased in tumor-bearing versus control WT mice (Figure 5J). Interestingly, Ces3/TGH deficiency attenuated VLDL production in control mice, but not in tumor-bearing mice (at least in the late stage of the experimental period; Figure 5J). Similar to WT mice, protein levels of Mttp were also unchanged in *Ces3/Tgh*$^{-/-}$ mice (Figure S5D). TG lipase (LPL plus hepatic lipase) activities were examined in post-heparin plasma (PHP) to assess the impact of tumors on peripheral VLDL clearance. In agreement with the FTT (Figure 2H), PHP TG lipase activities were significantly reduced in tumor-bearing WT mice (Figure 5K). A similar reduction conferred by tumor was also observed in *Ces3/Tgh*$^{-/-}$ mice (Figure 5K).

Restored Hepatic LDLR in *Ces3/Tgh*$^{-/-}$ Mice via Attenuation of PCSK9 Activation

Despite TPBC tumor-induced reduction of hepatic LDLR protein expression in both WT and *Ces3/Tgh*$^{-/-}$ mice, LDLR abundance was higher in tumor-bearing *Ces3/Tgh*$^{-/-}$ mice than in tumor-bearing WT mice (Figure 6A) and was independent of *Ldlr* transcription (Figure S6A). We therefore investigated the mechanism whereby Ces3/TGH deficiency results in augmented LDLR levels. In both genotypes, tumors increased plasma concentrations of PCSK9 (Figure 6B). However, plasma PCSK9 levels were significantly lower in *Ces3/Tgh*$^{-/-}$ mice than *WT* mice in both tumor-bearing and non-tumor conditions (Figure 6B). Concomitantly, we observed a positive correlation between tumor weight and plasma

PCSK9 levels in WT mice, but not in *Ces3/Tgh*$^{-/-}$ mice (Figure 6C). Hepatic *Pcsk9* mRNA expression was increased in tumor-bearing WT mice but unaltered in *Ces3/Tgh*$^{-/-}$ mice (Figure 6D). Expression of mRNA encoding hepatic nuclear factor α (*Hnf1a*), which is responsible for mammalian target of rapamycin complex 1 (mTORC1)-regulated transcriptional activation of the *Pcsk9* promoter (Ai et al., 2012), was increased in tumor-bearing WT mice, but not in *Ces3/Tgh*$^{-/-}$ mice when compared with their non-tumor counterparts (Figure 6E). Indeed, tumor burden tended to decline the phosphorylation of ribosomal protein S6, which reflects the activity of mTOCR1, in livers of fasted WT mice (Figure S6B) and serum-starved primary hepatocytes from non-fasted *WT* mice (Figure S6C). The activity of mTORC1 can be suppressed by cellular stress such as energy deprivation. Correspondingly, phosphorylation of the energy sensor 5′ AMP-activated protein kinase α (AMPKα) in liver was increased by 1.4-fold in tumor-bearing WT mice, whereas remained unchanged in tumor-bearing *Ces3/Tgh*$^{-/-}$ mice compared to respective non-tumor controls (Figure 6F). These data suggest that the activation of HNF1α/PCSK9 is responsible for reduced LDLR content in liver, which might be initiated by AMPK-mediated mTORC1 inhibition. However, the functional link between these factors still requires further confirmation.

Livers of tumor-bearing mice had an increased abundance of F4/80-positive macrophages (Kupffer cells) that was accompanied by increased proliferation rates of hepatocytes as determined by Ki67 staining (Figure 6G). Tumor-mediated liver enlargement was attenuated in *Ces3/Tgh*$^{-/-}$ mice (Figure 6H). This was also reflected by loss of the positive correlation between tumor and liver weight present in WT mice (Figure 6I). mRNA expression of pro-inflammatory markers (*Tnfa*, *Mcp1*, *F4/80*, and *Socs3*) in livers was markedly increased in tumor-bearing mice of both genotypes, whereas differences between genotypes were not significant (Figure S6D). Inflammatory stimuli (e.g., lipopolysaccharide [LPS]) induce *Pcsk9* expression and consequently LDLR degradation in mouse liver (Feingold et al., 2008). However, treatment of the immortalized hepatocyte cell line AML-12 with recombinant TNF-α, interleukin-6 (IL-6), and LPS failed to mimic the mRNA pattern of an induced PCSK9-LDLR axis and SREBPs in tumor-bearing mice (Figure S6E), suggesting an indirect inflammatory regulation of hepatic LDL clearance. Collectively, Ces3/TGH deficiency could alleviate tumor-induced liver enlargement, which might be ascribed to reduction of PCSK9-mediated degradation of LDLR.

Discussion

Metabolic reprogramming of lipid metabolism present in a wide range of cancers plays a critical role in the pathogenesis of human malignancies and cancer-associated cachexia. TG and cholesterol are hydrophobic molecules and must be transported in the circulation in lipoproteins. Aberrant lipoprotein profiles are often observed in cancer patients. Low plasma levels of TC and LDL-C, as well as high TG concentrations, are generally correlated with a high risk for various types of hematological and solid tumors (Fiorenza et al., 2000; Naik et al., 2006; Patel et al., 2004). In contrast, elevated plasma TC, LDL-C, and TG levels were observed in patients with breast cancer (Fiorenza et al., 2000). Despite the proposed association of cancer with low LDL-C, its bidirectional causalities with tumor development and the mechanisms involved are poorly understood and need further investigation. A

Mendelian randomization study showed that cancer risk in a population with spontaneous decrease of LDL-C resulting from polymorphisms in PCSK9, ABCG8, and ApoE is comparable with that in healthy subjects, suggesting that lower plasma LDL-C concentrations per se do not cause cancer (Benn et al., 2011). Notably, in prostate cancer, the reduction of plasma TC levels in patients with metastatic disease compared to non-metastatic patients and healthy men is associated with increased catabolism of LDL (Henriksson et al., 1989). Given that enriched circulating cholesterol provokes growth of breast and prostate tumor in mice (Alikhani et al., 2013; Zhuang et al., 2005), the reduction of plasma LDL-C in cancer is partially attributable to enhanced cholesterol uptake by tumors via LDLR. LDLR expression and its transcriptional regulation in tumors are largely unexplored. Here, based on human cancer data from TCGA, we found a robust correlation between *Ldlr* and *Srebp1* mRNA as well as *Srebp1*-regulated lipogenic enzymes for which pro-tumorigenic activities have been recently described (Arana et al., 2010; Currie et al., 2013; Lewis et al., 2015). This finding implies that LDLR and other lipogenic enzymes (e.g., SCD1 and FASN) play an important role in tumorigenesis. In support, supplementation of cells with VLDL and LDL reversed the pro-apoptotic effect conferred by LPDS. Supply of cholesterol alone could also stimulate cell proliferation. The tumor-supportive property of cholesterol might be due to its role in the maintenance of fluidity and permeability of the plasma membrane. Additionally, cholesterol is a major component of lipid rafts that have been reported to play a role in tumor signaling through recruitment of signaling components and initiation of distinct downstream signaling (Alikhani et al., 2013).

Our results suggest that tumor-induced increase in plasma VLDL concentration is partially due to enhanced secretion. FAs required for VLDL-TG synthesis during fasting are obtained from WAT lipolysis. TPBC tumors may influence systemic lipid mobilization through production of pro-inflammatory cytokines (e.g., TNF-α and IL-6; Huang et al., 2013). Elevated plasma TNF-α can drive FA efflux from WAT through enhanced lipolysis (Zhang et al., 2002). Despite unaltered de novo FA synthesis in liver, a substantial flow of FAs from WAT together with reduced hepatic FA oxidation likely ensures adequate provision of FAs for VLDL assembly in tumor-bearing mice. The observed accelerated esterification of extracellular FAs into TG and CE determined by a metabolic labeling assay might contribute to tumor-increased VLDL production.

Despite tumor-mediated attenuation of LPL activity, circulating LDL-C levels were increased due to reduced hepatic LDLR protein. Hepatic *Ldlr* expression is primarily regulated by SREBP2 in a cholesterol-dependent manner (Horton et al., 2003). In certain conditions, LDLR expression might also be under the control of SREBP1 (Sekar and Veldhuis, 2004; Streicher et al., 1996). In our TPBC model, hepatic SREBP1, but not 2, was reduced in tumor-bearing WT mice. However, downregulation of SREBP1 failed to downregulate *Ldlr* transcripts in mice, suggesting a potential post-translational regulation of LDLR independent of SREBP signaling.

Our study for the first time reports that B cell tumor dramatically induced expression of hepatic PCSK9 resulting in elevated plasma PCSK9 concentrations and reduced hepatic LDLR protein abundance. The tissue specificity of LDLR protein regulation by PCSK9 renders the liver the most responsive organ (Luo et al., 2009), eliminating adverse effects on

tumor LDLR-mediated VLDL remnant/LDL uptake and thus suppressing tumor growth. The *Pcsk9* proximal promoter contains a binding site for HNF1α, a liver-enriched transcription factor that cooperates with SREBP2 in the basal transcription of *PCSK9* (Li et al., 2009). In agreement, increased *Hnf1a* expression was detected in tumor-bearing WT mice. mTORC1-mediated repression of HNF1a and PCSK9 was reported to be involved in the maintenance of hepatic LDLR abundance (Ai et al., 2012). We observed a trend toward decreased mTORC1 activity in tumor-bearing WT mice. mTORC1 activity is negatively regulated by TSC1/2. Stress such as hypoxia, DNA damage, and energy deprivation activate TSC1/2 and thus repress mTORC1 signaling (Laplante and Sabatini, 2012). In livers of tumor-bearing mice, proliferation of hepatocytes together with suppression of FA oxidation conceptually results in energy deficit leading to activation of AMPK. AMPK was activated in tumor-bearing WT mice, supporting the involvement of tumor-mediated AMPK-mTORC1-HNF1α-PCSK9-LDLR signaling axis. Importantly, as a central regulator of cellular homeostasis and growth mTOR responds to various nutrients and stress. For instance, mTOR mediates insulin regulation of lipid metabolism, whereas it also impinges insulin sensitivity under various pathological conditions such as inflammation (Kim et al., 2008). It remains to be determined how these integrated networks converging on mTOR affect HNF1α-regulated expression of PCSK9 and LDLR in liver in distinct physiological and pathological settings. Hepatic PCSK9 expression can also be regulated by PPARα-mediated repression of *Pcsk9* promoter activity concomitantly with promotion of PCSK9 degradation (Kourimate et al., 2008). Suppressed PPARα signaling in TPBC tumor-bearing mice (Huang et al., 2013) might also have an influence on PCSK9 levels.

Interestingly, although hepatic *Pcsk9* expression was diminished in mice with LLC or B16 tumors, plasma PCSK9 concentrations were higher than in non-tumor controls. Increased plasma PCSK9 concentration might be due to binding of PCSK9 to LDL, which prevents clearance of circulating PCSK9 and degradation of LDLR (Kosenko et al., 2013). This might explain the observed unaltered hepatic LDLR protein abundance together with elevated concentrations of both PCSK9 and LDL in LLC and, to a lesser extent, in B16 tumor-bearing mice. PCSK9 binding to LDLR occurs either at the cell surface or in the trans-Golgi, leading to lysosomal degradation of both proteins (Lagace, 2014). The observed enhanced hepatic *Pcsk9* expression in TPBCs might contribute to LDLR reduction in liver, which is not observed in LLC or B16 tumor-bearing mice.

To further explore the cross-talk between lipids in the circulation and tumor progression, we investigated TPBC tumor associated effects in *Ces3/Tgh*$^{-/-}$ mice, a genetic hypolipidemic mouse model with attenuated VLDL secretion. Interestingly, tumor-mediated increase in circulating ApoB-containing lipoproteins and tumor growth were reduced in *Ces3/Tgh*$^{-/-}$ mice. Surprisingly, no attenuation of tumor-induced VLDL secretion in mice was observed on day 14 post-tumor inoculation, leading to the assumption that the attenuation of hyperlipidemia observed in tumor-bearing *Ces3/Tgh*$^{-/-}$ mice might be due to multiple mechanisms not solely to altered VLDL production. Nevertheless, it is conceivable that reduced VLDL secretion persists in the initial period of tumor growth, which might exert an inhibitory effect on proliferation and survival of TPBCs. In addition to enhanced VLDL production, CM and VLDL clearance was blunted in tumor-bearing mice, which also explains increased plasma TG levels. However, Ces3/TGH-deficient mice present with

upregulated LDL turnover due to reduced plasma PCSK9 concentrations in both non-tumor and tumor conditions compared to WT mice. In line with decreased PCSK9 activation, the upstream regulators AMPK and HNF1α were inactivated in *Ces3/Tgh*$^{-/-}$ mice. Consequently, hepatic LDLR is preserved in tumor-bearing *Ces3/Tgh*$^{-/-}$, but not WT mice. The alleviation of tumor-induced liver enlargement in tumor-bearing *Ces3/Tgh*$^{-/-}$ suggests that Ces3/TGH deficiency might protect mice against tumor-triggered liver dysfunction and consequently aberrant lipoprotein homeostasis.

In summary, we report that the decreased LPL-mediated hydrolysis of TG-rich lipoproteins together with enhanced VLDL production results in hypertriglyceridemia in tumor-bearing mice. In livers of tumor-bearing WT mice, PCSK9-mediated degradation of LDLR protein is mainly augmented by activation of hepatic PCSK9 and HNF1α, resulting in hypercholesterolemia. Hypertriglyceridemia and hypercholesterolemia in WT mice presumably provide tumors with essential exogenous lipids to support proliferation and protect against apoptosis. Diminishment of tumor-induced hyperlipidemia in *Ces3/Tgh*$^{-/-}$ mice leads to tumor suppression (Figure 7). Our experimental data confirm the existence of a tumor-associated positive feedback loop linking tumor progression and aberrant lipoprotein homeostasis in mice and offer supporting evidence for the importance of the “tumor macroenvironment” in the pathogenesis of cancer.

Experimental Procedures

Cells

Bcr/Abl-transformed precursor B cells (TPBCs) were generated as previously reported (Huang et al., 2013). Cells were maintained in RPMI 1640 medium containing 10% FBS (Life Technologies) in a 37°C incubator with 5% CO_2. Cell number and viability was determined using CASY cell counter (Schaä rfe System).

mRNA Expression Analysis and RNA Sequencing

Total RNA was extracted by Trizol (Life Technologies). cDNA was synthesized from 2 mg total RNA by the Superscript III Reverse Transcriptase (Invitrogen) using oligo $(dT)_{12–18}$ primers. Real-time qPCR was performed with the Platinum SYBR Green qPCR SuperMix-UDG kit (Invitrogen) in the Rotor-Gene 3000 instrument (Montreal Biotech). Primers used in this study are listed in Table S2. Gene expression profile in TPBCs was determined by a quantitative RNA-sequencing analysis on the Ion Torrent platform (Thermo Fisher Scientific).

Immunoblotting

Immunoblotting was performed using total or fractionated protein extracts (subcellular fractionation described in Supplemental Experimental Procedures) or plasma and probed with antibodies listed above. Immunoreactivity was detected by ECL (Amersham-Pharmacia) or SuperSignal West Dura (Thermo Fisher Scientific) to enhance the signal. Immunoblots were scanned and quantified using G-Box (Syngene).

Animals

All animal experiments were approved by the University of Alberta Animal Care and Use Committee and were performed in accordance with the guidelines of the Canadian Council on Animal Care. Mice were maintained on 12-hr light:-dark cycles and fed a standard chow diet. All wild-type and *Ces3/Tgh*$^{-/-}$ mice were of C57BL/6J genetic background. Twelve to 15 week-old male mice were randomly divided into groups. TPBCs (200,000 per mouse), LLC (2,000,000), and B16 (1,500,000) were injected subcutaneously into mice in the flank. Control treatment mice received vehicle (PBS). Three dimensions of tumors were measured by caliper, and tumor volume was estimated based on the formula "1/2 × length × width × height." Non-fasting, fasting, and refeeding regimens were applied. "Non-fasting" indicates withdrawal of food during daytime (8 a.m. to 1 p.m.) with minimal dietary stress to mice. "Fasting" denotes 16-hr overnight removal of food (6 p.m. to 10 a.m.). "Refeeding" indicates overnight fasting plus food supply with chow diet for the following 12 hr. Mice were sacrificed under anesthesia with isoflurane, and blood was collected by retrobulbar bleeding.

PHP TG Lipase Activity Assay

PHP was drawn 20 min after subcutaneous injection of sodium heparin (500 U/kg body weight). Enzyme activities of LPL and hepatic lipase in PHP were assayed as previously described (Zechner, 1990).

Hepatic VLDL Secretion

Mice were fasted overnight followed by subcutaneous injection with P-407 (1 mg/g body weight) to inhibit peripheral lipolysis. Plasma samples were drawn right before P-407 injection as an initial time point and 1, 2, and 3 hr after injection. Plasma TG concentration at each time point was determined.

Metabolic Labeling Studies in Primary Hepatocytes

Primary hepatocytes were isolated from non-fasted mice by perfusion with 0.8 mg/mL Collagenase Type I (Worthington Biochemical Group, NJ) through the portal vein. Cells were incubated with DMEM containing 15% FBS for 4 hr for cell attachment as described previously (Wei et al., 2010). For incorporation of exogenous substrates into lipids, hepatocytes were washed twice, and then incubated for 4 hr in 2 ml serum-free DMEM containing either 5 μCi [^{3}H] oleate (combined with 400 μM oleate conjugated with 0.5% FA-free BSA) or 5 μCi [^{3}H] acetate (combined with 50 μM sodium acetate). Cells and media (after washing with PBS to remove unabsorbed substrate) were collected for analysis (pulse) or incubated with DMEM for further 12 hr (chase). [^{3}H]-labeled lipids were determined following lipid extraction and thin-layer chromatography by liquid scintillation counting as described above.

Statistical Analyses

Data are presented as mean ± SEM. Statistical analysis was performed using GraphPad Prism5. Unpaired Student's two-tailed t test and ANOVA followed by Bonferroni posttest were used to determine significance of differences between groups where appropriate.

Correlation was studied by Pearson's correlation test or Spearman's correlation as indicated. Values of $p < 0.05$ were considered as significantly different.

Supplemental Information

Refer to Web version on PubMed Central for supplementary material.

Acknowledgments

We would like to thank Drs. Michael Brown and Joseph Goldstein for anti-SREBP1c antibodies and Dr. Russell DeBose-Boyd for anti-HMGCoAR antibodies; Russell Watts, Randal Nelson, Dr. Elke Stadelmeyer, and Anton Ibovnik for additional technical assistance; and Dr. Martina Schweiger for fruitful discussions. We are also grateful to Dr. Da-wei Zhang for PCSK9 and LDLR discussions. We thank Dr. Ing Swie Goping and Dr. Rene´ Jacobs for manuscript editing. Some analyses were performed by the Lipidomics Core Facility at the University of Alberta Faculty of Medicine and Dentistry, which receives support from the Women and Children Health Research Institute. This work was supported by grants from the Canadian Institutes of Health Research (MOP-69043 to R.L.), the Austria Science Fund (FWF) projects W1226 DK Metabolic and Cardiovascular Disease and SFB LIPOTOX F30 (to G.H. and D.K.), and the European Research Council Advanced Grant LIPOCHEX (to P.W.V.).

References

Ai D, Chen C, Han S, Ganda A, Murphy AJ, Haeusler R, Thorp E, Accili D, Horton JD, Tall AR. Regulation of hepatic LDL receptors by mTORC1 and PCSK9 in mice. J Clin Invest. 2012; 122:1262–1270. [PubMed: 22426206]

Al-Zoughbi W, Huang J, Paramasivan GS, Till H, Pichler M, Guertl-Lackner B, Hoefler G. Tumor macroenvironment and metabolism. Semin Oncol. 2014; 41:281–295. [PubMed: 24787299]

Alikhani N, Ferguson RD, Novosyadlyy R, Gallagher EJ, Scheinman EJ, Yakar S, LeRoith D. Mammary tumor growth and pulmonary metastasis are enhanced in a hyperlipidemic mouse model. Oncogene. 2013; 32:961–967. [PubMed: 22469977]

Arana L, Gangoiti P, Ouro A, Trueba M, Gómez-Muñoz A. Ceramide and ceramide 1-phosphate in health and disease. Lipids Health Dis. 2010; 9:15. [PubMed: 20137073]

Benn M, Tybjærg-Hansen A, Stender S, Frikke-Schmidt R, Nordest-gaard BG. Low-density lipoprotein cholesterol and the risk of cancer: a mendelian randomization study. J Natl Cancer Inst. 2011; 103:508–519. [PubMed: 21285406]

Bianchini F, Kaaks R, Vainio H. Overweight, obesity, and cancer risk. Lancet Oncol. 2002; 3:565–574. [PubMed: 12217794]

Calle EE, Rodriguez C, Walker-Thurmond K, Thun MJ. Overweight, obesity, and mortality from cancer in a prospectively studied cohort of U.S. adults. N Engl J Med. 2003; 348:1625–1638. [PubMed: 12711737]

Currie E, Schulze A, Zechner R, Walther TC, Farese RV Jr. Cellular fatty acid metabolism and cancer. Cell Metab. 2013; 18:153–161. [PubMed: 23791484]

Dolinsky VW, Douglas DN, Lehner R, Vance DE. Regulation of the enzymes of hepatic microsomal triacylglycerol lipolysis and re-esterification by the glucocorticoid dexamethasone. Biochem J. 2004a; 378:967–974. [PubMed: 14662008]

Dolinsky VW, Gilham D, Alam M, Vance DE, Lehner R. Triacylglycerol hydrolase: role in intracellular lipid metabolism. Cell Mol Life Sci. 2004b; 61:1633–1651. [PubMed: 15224187]

Feingold KR, Moser AH, Shigenaga JK, Patzek SM, Grunfeld C. Inflammation stimulates the expression of PCSK9. Biochem Biophys Res Commun. 2008; 374:341–344. [PubMed: 18638454]

Fiorenza AM, Branchi A, Sommariva D. Serum lipoprotein profile in patients with cancer. A comparison with non-cancer subjects. Int J Clin Lab Res. 2000; 30:141–145. [PubMed: 11196072]

Guillaumond F, Bidaut G, Ouaissi M, Servais S, Gouirand V, Olivares O, Lac S, Borge L, Roques J, Gayet O, et al. Cholesterol uptake disruption, in association with chemotherapy, is a promising combined metabolic therapy for pancreatic adenocarcinoma. Proc Natl Acad Sci USA. 2015; 112:2473–2478. [PubMed: 25675507]

Europe PMC Funders Author Manuscripts

Guo D, Reinitz F, Youssef M, Hong C, Nathanson D, Akhavan D, Kuga D, Amzajerdi AN, Soto H, Zhu S, et al. An LXR agonist promotes glioblastoma cell death through inhibition of an EGFR/AKT/SREBP-1/LDLR-dependent pathway. Cancer Discov. 2011; 1:442–456. [PubMed: 22059152]

Henriksson P, Eriksson M, Ericsson S, Rudling M, Stege R, Berglund L, Angelin B. Hypocholesterolaemia and increased elimination of low-density lipoproteins in metastatic cancer of the prostate. Lancet. 1989; 2:1178–1180. [PubMed: 2572901]

Horton JD, Bashmakov Y, Shimomura I, Shimano H. Regulation of sterol regulatory element binding proteins in livers of fasted and refed mice. Proc Natl Acad Sci USA. 1998; 95:5987–5992. [PubMed: 9600904]

Horton JD, Shah NA, Warrington JA, Anderson NN, Park SW, Brown MS, Goldstein JL. Combined analysis of oligonucleotide micro-array data from transgenic and knockout mice identifies direct SREBP target genes. Proc Natl Acad Sci USA. 2003; 100:12027–12032. [PubMed: 14512514]

Huang J, Das SK, Jha P, Al Zoughbi W, Schauer S, Claudel T, Sexl V, Vesely P, Birner-Gruenberger R, Kratky D, et al. The PPARα agonist fenofibrate suppresses B-cell lymphoma in mice by modulating lipid metabolism. Biochim Biophys Acta. 2013; 1831:1555–1565. [PubMed: 23628473]

Kim JH, Kim JE, Liu HY, Cao W, Chen J. Regulation of interleukin-6-induced hepatic insulin resistance by mammalian target of rapamycin through the STAT3-SOCS3 pathway. J Biol Chem. 2008; 283:708–715. [PubMed: 17993646]

Kosenko T, Golder M, Leblond G, Weng W, Lagace TA. Low density lipoprotein binds to proprotein convertase subtilisin/kexin type-9 (PCSK9) in human plasma and inhibits PCSK9-mediated low density lipoprotein receptor degradation. J Biol Chem. 2013; 288:8279–8288. [PubMed: 23400816]

Kourimate S, Le May C, Langhi C, Jarnoux AL, Ouguerram K, Zaïr Y, Nguyen P, Krempf M, Cariou B, Costet P. Dual mechanisms for the fibrate-mediated repression of proprotein convertase subtilisin/kexin type 9. J Biol Chem. 2008; 283:9666–9673. [PubMed: 18245819]

Kuemmerle NB, Rysman E, Lombardo PS, Flanagan AJ, Lipe BC, Wells WA, Pettus JR, Froehlich HM, Memoli VA, Morganelli PM, et al. Lipoprotein lipase links dietary fat to solid tumor cell proliferation. Mol Cancer Ther. 2011; 10:427–436. [PubMed: 21282354]

Lagace TA. PCSK9 and LDLR degradation: regulatory mechanisms in circulation and in cells. Curr Opin Lipidol. 2014; 25:387–393. [PubMed: 25110901]

Laplante M, Sabatini DM. mTOR signaling in growth control and disease. Cell. 2012; 149:274–293. [PubMed: 22500797]

Lewis CA, Brault C, Peck B, Bensaad K, Griffiths B, Mitter R, Chakravarty P, East P, Dankworth B, Alibhai D, et al. SREBP maintains lipid biosynthesis and viability of cancer cells under lipid- and oxygen-deprived conditions and defines a gene signature associated with poor survival in glioblastoma multiforme. Oncogene. 2015; 34:5128–5140. [PubMed: 25619842]

Li H, Dong B, Park SW, Lee HS, Chen W, Liu J. Hepatocyte nuclear factor 1alpha plays a critical role in PCSK9 gene transcription and regulation by the natural hypocholesterolemic compound berberine. J Biol Chem. 2009; 284:28885–28895. [PubMed: 19687008]

Lian J, Quiroga AD, Li L, Lehner R. Ces3/TGH deficiency improves dyslipidemia and reduces atherosclerosis in Ldlr(-/-) mice. Circ Res. 2012a; 111:982–990. [PubMed: 22872154]

Lian J, Wei E, Wang SP, Quiroga AD, Li L, Di Pardo A, van der Veen J, Sipione S, Mitchell GA, Lehner R. Liver specific inactivation of carboxylesterase 3/triacylglycerol hydrolase decreases blood lipids without causing severe steatosis in mice. Hepatology. 2012b; 56:2154–2162. [PubMed: 22707181]

Louie SM, Roberts LS, Mulvihill MM, Luo K, Nomura DK. Cancer cells incorporate and remodel exogenous palmitate into structural and oncogenic signaling lipids. Biochim Biophys Acta. 2013; 1831:1566–1572. [PubMed: 23872477]

Luo Y, Warren L, Xia D, Jensen H, Sand T, Petras S, Qin W, Miller KS, Hawkins J. Function and distribution of circulating human PCSK9 expressed extrahepatically in transgenic mice. J Lipid Res. 2009; 50:1581–1588. [PubMed: 19060325]

Naik PP, Ghadge MS, Raste AS. Lipid profile in leukemia and Hodgkin's disease. Indian J Clin Biochem. 2006; 21:100–102. [PubMed: 23105623]

Patel PS, Shah MH, Jha FP, Raval GN, Rawal RM, Patel MM, Patel JB, Patel DD. Alterations in plasma lipid profile patterns in head and neck cancer and oral precancerous conditions. Indian J Cancer. 2004; 41:25–31. [PubMed: 15105576]

Sekar N, Veldhuis JD. Involvement of Sp1 and SREBP-1a in transcriptional activation of the LDL receptor gene by insulin and LH in cultured porcine granulosa-luteal cells. Am J Physiol Endocrinol Metab. 2004; 287:E128–E135. [PubMed: 14998783]

Sjöström L, Gummesson A, Sjöström CD, Narbro K, Peltonen M, Wedel H, Bengtsson C, Bouchard C, Carlsson B, Dahlgren S, et al. Swedish Obese Subjects Study. Effects of bariatric surgery on cancer incidence in obese patients in Sweden (Swedish Obese Subjects Study): a prospective, controlled intervention trial. Lancet Oncol. 2009; 10:653–662. [PubMed: 19556163]

Streicher R, Kotzka J, Müller-Wieland D, Siemeister G, Munck M, Avci H, Krone W. SREBP-1 mediates activation of the low density lipoprotein receptor promoter by insulin and insulin-like growth factor-I. J Biol Chem. 1996; 271:7128–7133. [PubMed: 8636148]

Vitols S, Angelin B, Ericsson S, Gahrton G, Juliusson G, Masquelier M, Paul C, Peterson C, Rudling M, Söderberg-Reid K, et al. Uptake of low density lipoproteins by human leukemic cells in vivo: relation to plasma lipoprotein levels and possible relevance for selective chemotherapy. Proc Natl Acad Sci USA. 1990; 87:2598–2602. [PubMed: 2320578]

Vitols S, Peterson C, Larsson O, Holm P, Aberg B. Elevated uptake of low density lipoproteins by human lung cancer tissue in vivo. Cancer Res. 1992; 52:6244–6247. [PubMed: 1423268]

Wei E, Ben Ali Y, Lyon J, Wang H, Nelson R, Dolinsky VW, Dyck JR, Mitchell G, Korbutt GS, Lehner R. Loss of TGH/Ces3 in mice decreases blood lipids, improves glucose tolerance, and increases energy expenditure. Cell Metab. 2010; 11:183–193. [PubMed: 20197051]

Zechner R. Rapid and simple isolation procedure for lipoprotein lipase from human milk. Biochim Biophys Acta. 1990; 1044:20–25. [PubMed: 2340307]

Zhang HH, Halbleib M, Ahmad F, Manganiello VC, Greenberg AS. Tumor necrosis factor-alpha stimulates lipolysis in differentiated human adipocytes through activation of extracellular signal-related kinase and elevation of intracellular cAMP. Diabetes. 2002; 51:2929–2935. [PubMed: 12351429]

Zhuang L, Kim J, Adam RM, Solomon KR, Freeman MR. Cholesterol targeting alters lipid raft composition and cell survival in prostate cancer cells and xenografts. J Clin Invest. 2005; 115:959–968. [PubMed: 15776112]

Europe PMC Funders Author Manuscripts

Europe PMC Funders Author Manuscripts

Highlights

- Lipoprotein cholesterol supports tumor growth
- Tumors increase VLDL/LDL levels
- Ces3/TGH deficiency attenuates tumor-induced hyperlipidemia via inhibition of PCSK9
- Tumor growth was suppressed in *Ces3/Tgh*$^{-/-}$ mice

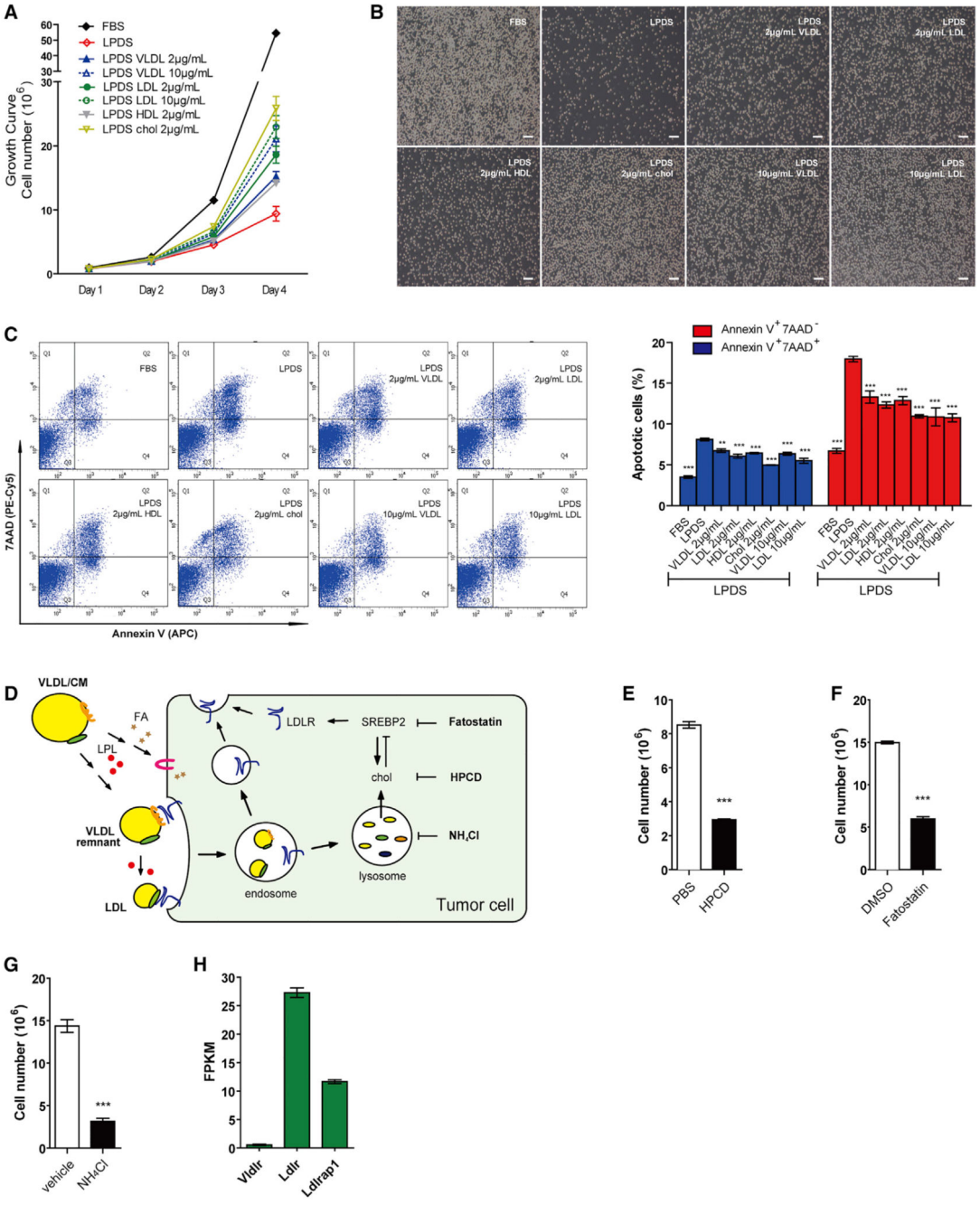

Figure 1. Lipoproteins Are Essential for Growth and Survival of Transformed B Cells

(A) Growth curve of TPBCs cultured in RPMI 1640 medium containing 10% FBS or LPDS medium supplemented with 2 or 10 μg/ml cholesterol in forms of VLDL, LDL, HDL, and cholesterol.

(B) Morphology of TPBC from (A; day 4). Scale bar, 200 μm.

(C) Determination of apoptotic cells by flow cytometry after 48 hr. Annexin V and 7AAD used as early and late stage apoptotic markers, respectively. The symbol (*) indicates significantly different from the LPDS group.

(D) Schematic representation of various reagents modifying cholesterol (Chol) metabolism reported in (E)–(G) and tumor-expressing transporters shown in (H).

(E) Impact of cellular cholesterol depletion by1%hydroxypropyl-β-cyclodextrin (HPCD) on growth of TPBCs. Cells were treated with HPCD for 20 min followed by culture in 10% LPDS medium for 40 hr.

(F and G) Impact of fatostatin (5 μM in 5% FBS medium) (F) and NH_4Cl (20 mM in 10% FBS medium) (G) treatment for 36 hr on cell growth.

(H) RNA-sequencing analysis of lipoprotein transporters (*Vldlr* and *Ldlr*) and related protein (*Ldlrap1*) in TPBCs.

Data (n = 3) are representative of two independent experiments. Error bars represent SEM; **p < 0.01 and ***p < 0.001 (unpaired t test). See also Figure S1.

Europe PMC Funders Author Manuscripts

Europe PMC Funders Author Manuscripts

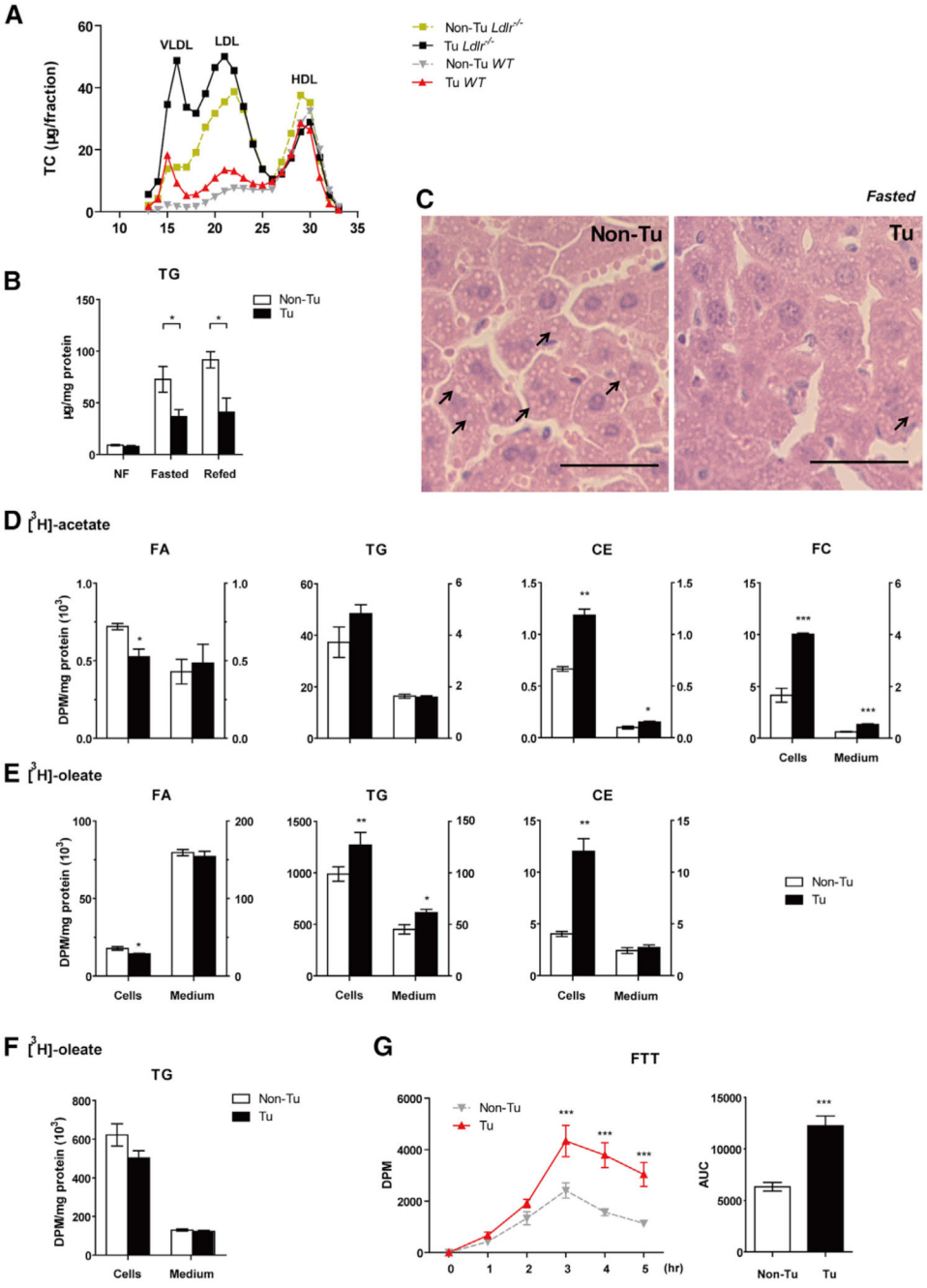

Figure 2. TPBC Tumors Increase VLDL Production and Decrease CM/VLDL Turnover

(A) TC concentrations in plasma after lipoprotein separation by FPLC in *WT* and *Ldlr*$^{-/-}$ mice (14 days post-injection, pooled from five mice each).

(B) Liver TG levels from non-fasted (NF; mice were fed overnight, but food was withdrawn from 8 a.m. to 1 p.m.), overnight (o/n)-fasted and refed (10 hr) WT mice with/without tumors (day 14, n = 4–5).

(C) Histological aspect of liver specimen from o/n fasted *WT* mice stained with H&E (n = 3). Scale bar, 10 µm.

(D and E) Primary hepatocytes were isolated from tumor-bearing (Tu) WT mice 13 days post-injection of TPBC tumor cells. Cells were incubated with [^{3}H]acetate (D) or [^{3}H] oleate (E) as substrates for “Pulse.”

(F) Cells were incubated with [^{3}H] oleate, washed, and then chased with serum-free DMEM. Radioactivity in distinct lipid species resolved by thin-layer chromatography (TLC) was counted. Data (n = 3) are representative of four independent experiments.

(G) Fat tolerant test (FTT) was performed in tumor-bearing (Tu)/control (Non-Tu) *WT* mice (day 14). Blood samples were collected and lipids were separated by TLC. Radioactivity in TG fraction was counted (n = 7). Statistic differences at different time points were determined by two-way ANOVA.

Error bars represent SEM. *$p < 0.05$, **$p < 0.01$, and ***$p < 0.001$ (unpaired t test, if not stated otherwise). See also Figure S2.

Europe PMC Funders Author Manuscripts

Europe PMC Funders Author Manuscripts

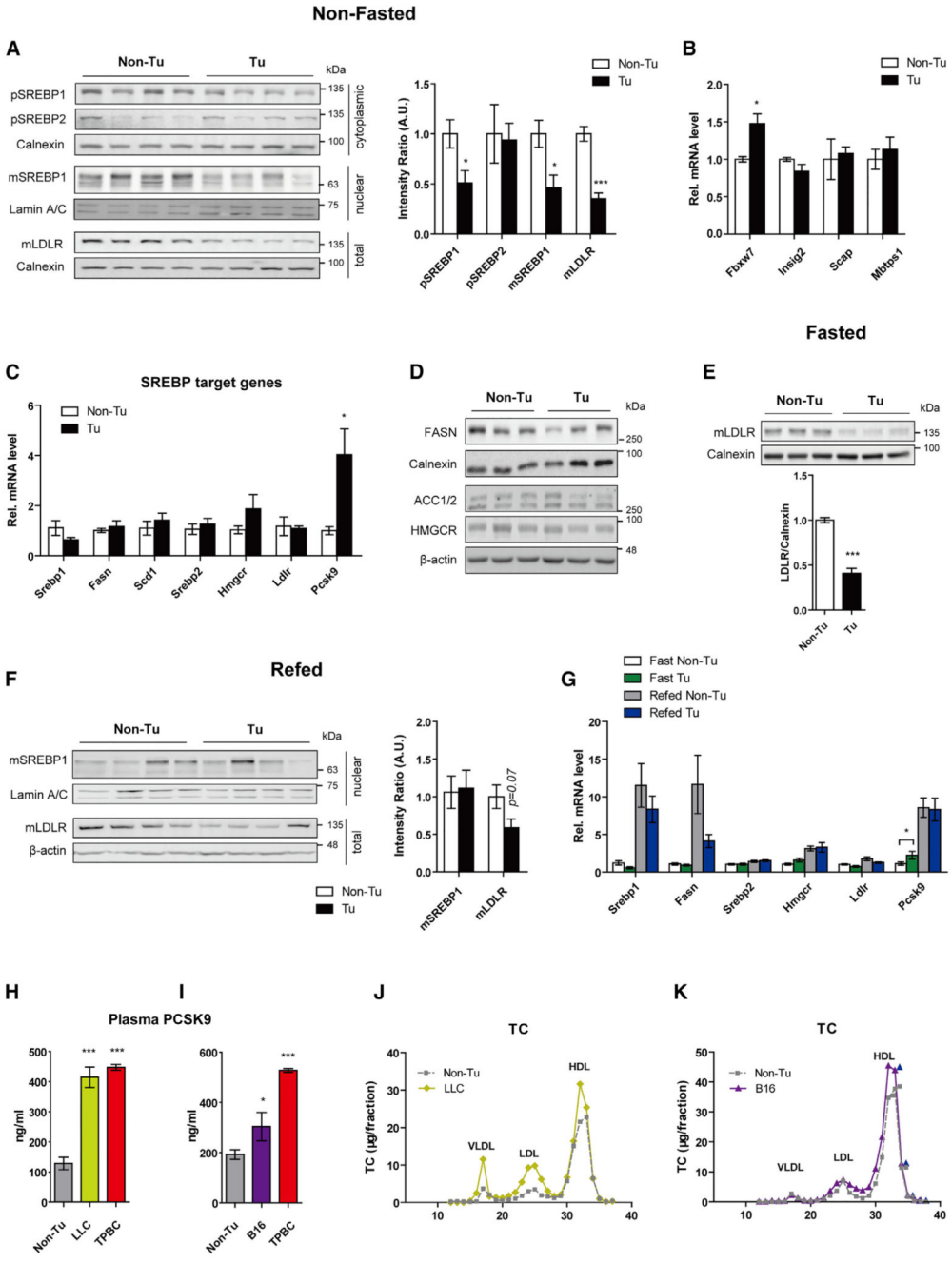

Figure 3. TPBC Tumors Decrease Hepatic LDLR Protein Expression, but Not Its Transcription

(A) Immunoblot analysis of hepatic SREBP1/2 precursor (pSREBP1/2; 125 kDa), mature SREBP1 (mSREBP1, 65-68 kDa), and mature LDLR (mLDLR, 130 kDa) in non-fasted WT mice 14 day post-injection. Loading control: Lamin A/C (70 kDa, nuclear fraction); Calnexin (90 kDa, cytosolic fraction and total) (n = 4).

(B and C) Hepatic transcriptional levels of genes involved in SREBP ubiquitination and processing (B) and *Srebp1/2* and their target genes (C) (non-fasted mice, n = 5) relative to cyclophilin A mRNA expression.

(D) Immunoblot analysis of FASN (273 kDa), ACC1/2 (265/280 kDa) and HMGCR (95 kDa), Calnexin and β-actin (45 kDa) in liver tissues from non-fasted mice (n = 3) were used as loading controls.
(E and F) Immunoblot analysis of hepatic mSREBP1 and mLDLR in o/n fasted (n = 3) and refed (n = 4) mice.
(G) Hepatic expression *Srebp1/2* and SREBP1/2 target genes during fasting and refeeding (n = 5).
(H and I) Plasma concentration of PCSK9 in LLC- (21 days) and TPBC-bearing (14 days) female mice and in B16- (17 days) and TPBC-bearing (14 days) male mice.
(J and K) TC concentrations in plasma lipoproteins separated by FPLC (plasma pooled from five mice) in non-tumor (Non-Tu) control, LLC mice, and B16 mice.
Error bars represent SEM. *p < 0.05 and ***p < 0.001 (unpaired t test). See also Figure S3.

Europe PMC Funders Author Manuscripts

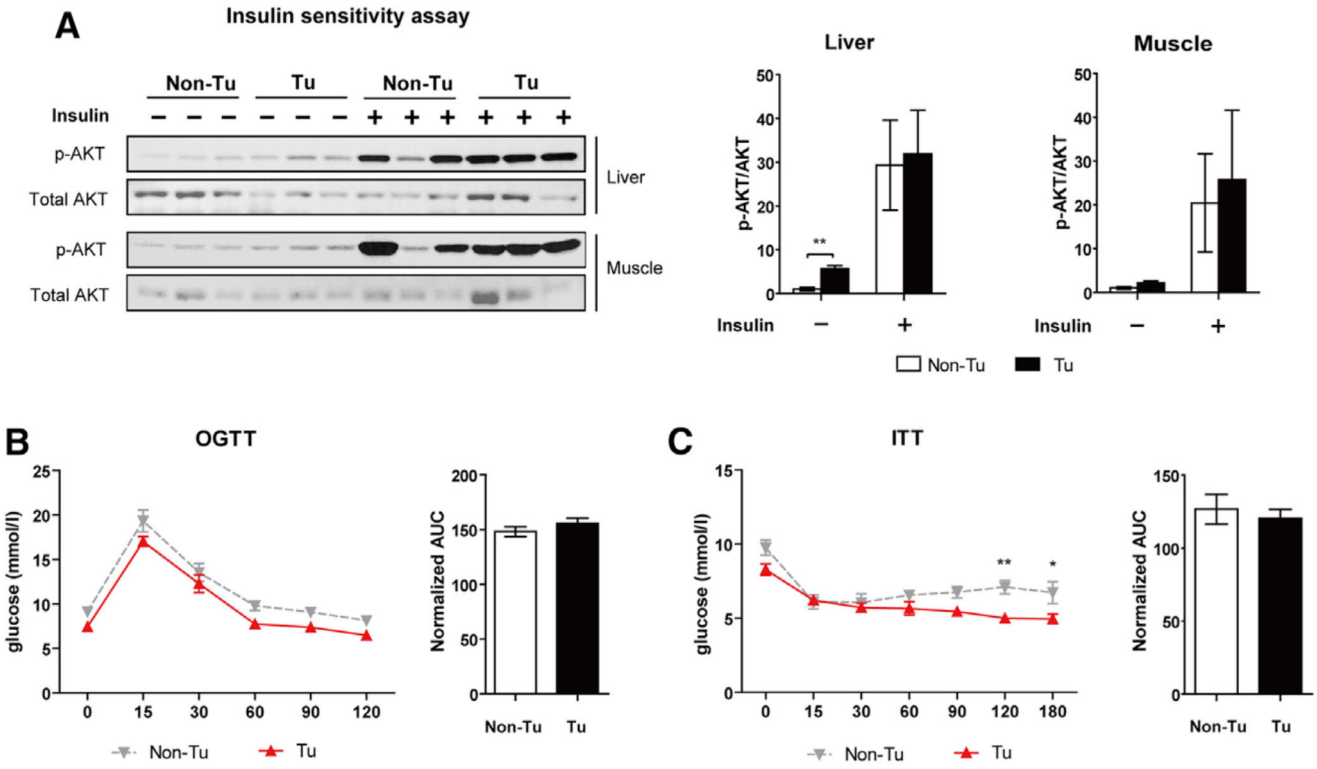

Figure 4. Unaltered Insulin Sensitivity in TPBC Tumor-Induced Hyperlipidemia

(A) Insulin sensitivity was assessed in livers and muscles of o/n-fasted mice (tumor-bearing [Tu]/control [Non-Tu]) on day 13 post-injection (n = 3). Total Akt and Ser473 phosphorylated (p-) AKT were probed by immunoblotting.

(B) Oral glucose tolerance test (OGTT) in o/n-fasted mice (day 12 post-injection, n = 7).

(C) Insulin tolerance test (ITT) in non-fasted mice (day 12 post-injection, n = 6).

Statistical differences at different time points were determined by two-way ANOVA. Area under curve (AUC) was normalized with the corresponding value at initial time point. Error bars represent SEM. *$p < 0.05$ and **$p < 0.01$ (unpaired t test, unless indicated otherwise). See also Figure S4.

Europe PMC Funders Author Manuscripts

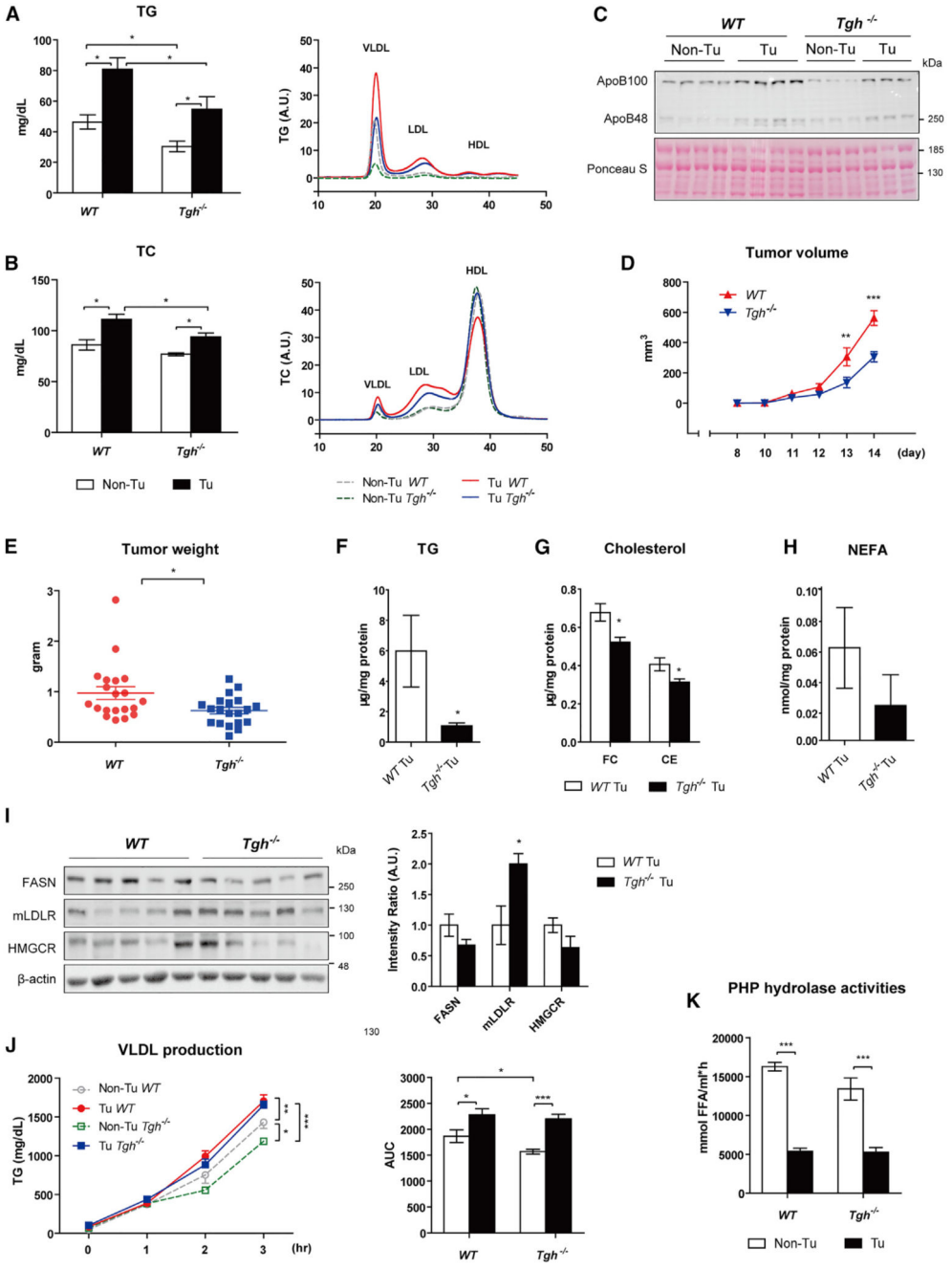

Figure 5. Ces3/TGH Deficiency Attenuates TPBC Tumor-Induced Hyperlipidemia and Tumor Growth

(A and B) Total plasma and lipoprotein TG (A) and TC (B) levels from non-fasted WT, *Ces3/Tgh*$^{-/-}$ mice (day 14 post-inoculation, n = 12). Bar graphs show the levels of total plasma TG and TC, while line graphs depict lipoprotein profiles by FPLC (plasma pooled from five mice).

(C) Immunoblot analysis of plasma ApoB100 (509 kDa) and ApoB48 (250 kDa). Ponceau S staining served as loading control.

(D) Tumor volume measured by caliper during the experiment (n = 12); two-way ANOVA.

(E) Tumor weight (day 14, n = 12).
(F–H) Quantification of TG (F), FC and CE (G), and NEFA (H) concentrations in tumors of WT and *Ces3/Tgh*$^{-/-}$ mice (day 14 post-inoculation, n = 6).
(I) Immunoblot analysis of FASN, mLDLR, and HMGCR in tumor lysates (n = 5).
(J) VLDL secretion rates in o/n fasted control (Non-Tu) and tumor-bearing (Tu) *WT* and *Ces3/Tgh*$^{-/-}$ mice (day 13 post-inoculation, n = 5−6). Plasma TG concentrations were determined before P-407 injection as initial time point and 1, 2, and 3 hr after injection; two-way ANOVA.
(K) TG lipase activities in post-heparin plasma (PHP) from tumor-bearing (Tu)/control (Non-Tu) *WT* and *Ces3/Tgh*$^{-/-}$ mice 14 days post-inoculation (n = 7).
Error bars represent SEM. *p < 0.05, **p < 0.01, and ***p < 0.001 (unpaired t test, unless indicated otherwise). See also Figure S5.

Europe PMC Funders Author Manuscripts

Europe PMC Funders Author Manuscripts

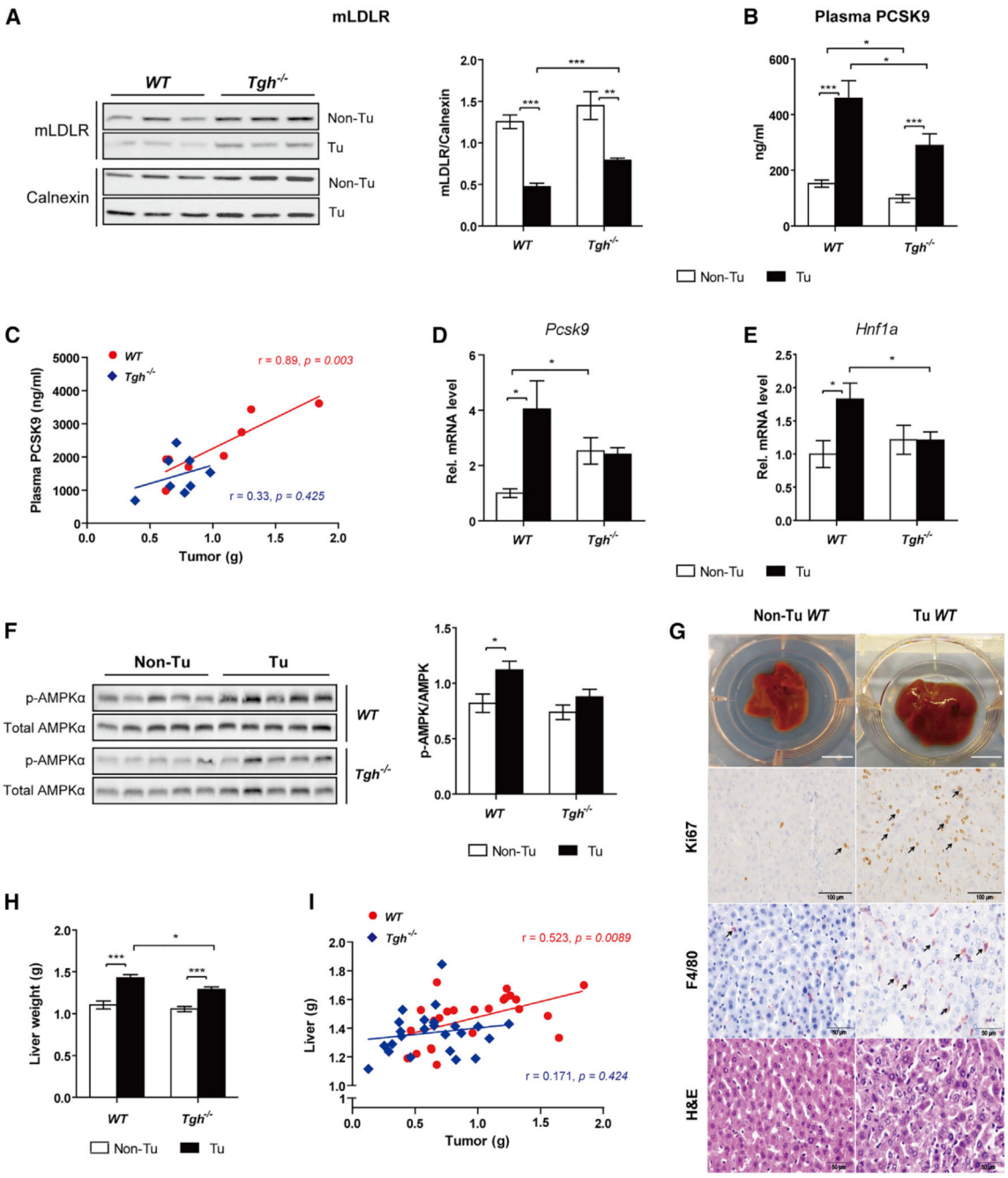

Figure 6. *Ces3/Tgh*$^{-/-}$ Mice Partially Restore Hepatic LDLR Expression via PCSK9 Inhibition

(A) Immunoblot analysis of LDLR protein levels in livers of WT and *Ces3/Tgh*$^{-/-}$ mice 14 days post-injection in non-fasted conditions (n = 5). Calnexin served as internal reference.

(B) PCSK9 plasma levels in control (Non-Tu)/tumor-bearing (Tu) WT and *Ces3*/*Tgh*$^{-/-}$ mice determined by ELISA assay (n = 8).

(C) Correlations between plasma PCSK9 concentration and tumor size in WT and *Ces3*/*Tgh*$^{-/-}$ mice were studied using a Pearson correlation coefficient test (n = 8).

(D and E) mRNA expression of hepatic *Pcsk9* (D) and *Hnf1a* (E) mRNA levels (n = 5–7).

(F) AMPK immunoblot analysis of Thr172 phosphorylated(p-)/total AMPKα (62 kDa; n = 5–7) from livers of WT and *Ces3*/*Tgh*$^{-/-}$ mice.

(G) Macroscopic views of whole livers (top), representative images of IHC staining for Ki67 (proliferation marker, second panel) and F4/80 (macrophage marker, third panel), H&E staining (bottom) in liver specimens are shown. Scale bars represent 10 mm (macroscopic images), 100 μm (Ki67), and 50 μm (F4/80 and H&E). Arrows indicate positive immunohistochemistry staining.

(H) Liver weight from control (Non-Tu)/tumor-bearing (Tu) WT and *Ces3*/*Tgh*$^{-/-}$ mice (n = 10–13).

(I) Correlation between tumor weights and liver weights in WT (n = 24) and *Ces3*/*Tgh*$^{-/-}$ mice (n = 24) by a Pearson correlation coefficient test. Error bars represent SEM. *p < 0.05, **p < 0.01, and ***p < 0.001 (unpaired t test unless indicated otherwise). See also Figure S6.

Europe PMC Funders Author Manuscripts

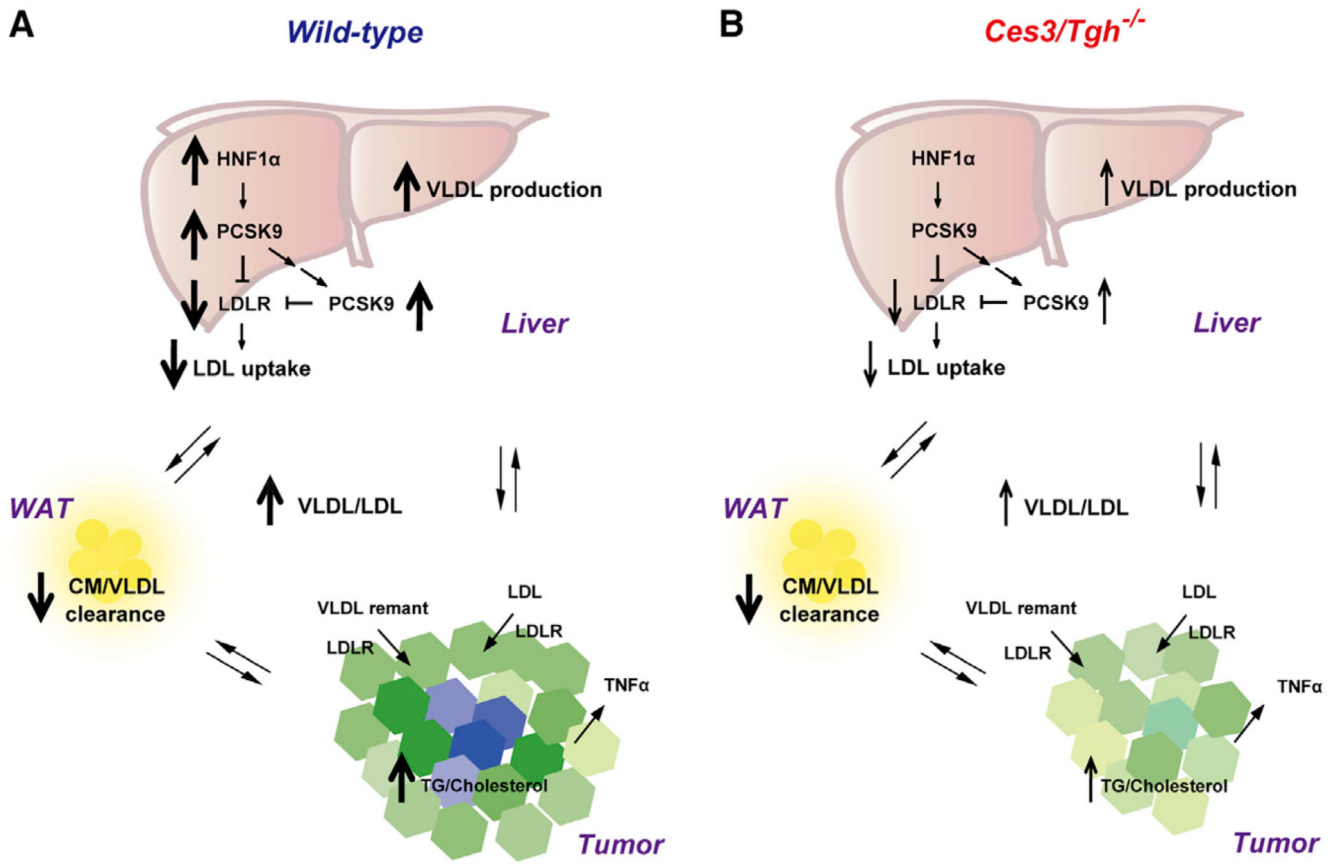

Figure 7. Schematic Model of Tumor Impact on Lipoprotein Homeostasis

(A) In WT mice, inhibition of TG-rich lipoprotein turnover in peripheral organs (e.g., WAT), together with stimulation of VLDL secretion from liver, contributes to TPBC tumor-increased plasma VLDL. Enhanced PCSK9-mediated LDLR degradation in liver causes insufficient LDL turnover and results in the elevation of plasma LDL. Hyperlipidemia thereby provides adequate amount of tumorigenic lipids, especially cholesterol, for tumor progression.

(B) In *Ces3/Tgh*$^{-/-}$ mice, despite lack of prevention against tumor-reduced VLDL/CM turnover and tumor-enhanced VLDL secretion, hypotriglyceridemia induced by Ces3/TGH deficiency-reduced VLDL production at the initial time, together with improvement of hepatic LDL uptake due to downregulation of hepatic *Pcsk9* expression, leading to reduced lipoprotein supply and suppression of tumor growth.

Europe PMC Funders Author Manuscripts